Drying method determines the structure and the solubility of microfluidized pea globulin aggregates

Bonastre Oliete, Salim A. Yassine, Eliane Cases, Rémi Saurel

Drying method determines the structure and the solubility of microfluidized pea globulin aggregates

Bonastre Oliete, Salim A. Yassine, Cases, E., Saurel, R.*

Univ. Bourgogne Franche-Comté, AgroSup Dijon, PAM UMR A 02.102, F-21000 Dijon, France

Bonastre Oliete: bonastre.oliete@u-bourgogne.fr

Salim A. Yassine: salimyassine007@yahoo.fr

Eliane Cases: eliane.cases@agrosupdijon.fr

*Rémi Saurel: Corresponding author: remi.saurel@grosupdijon.fr

Abstract

The effects of microfluidization and drying method on the characteristics and techno-functional properties of pea (*Pisum sativum L.*) globulin aggregates were investigated. Pea globulin aggregates were microfluidized at 130 MPa and spray-dried or freeze-dried thereafter. Microfluidization decreased aggregate size and surface hydrophobicity due to protein re-arrangements. Microfluidized pea globulin aggregates showed higher solubility but less suspension stability than non-microfluidized aggregates. Drying favored the re-aggregation of pea globulins with modifications in secondary structure of proteins more marked for spray-drying, decreased surface hydrophobicity and solubility, but increased suspension stability. Spray-dried aggregates were smaller than freeze-dried, with improved suspension stability. These results indicated that microfluidization and drying determine the structure of pea globulin aggregates and their associated techno-functional properties. These findings are crucial for the preparation of plant protein powders in the food industry.

Keywords: Pea globulin, Aggregate, Microfluidization, High dynamic pressure, Spray-drying, Freeze-drying, Microscopy, Structure, Solubility, Suspension stability

1. Introduction

The use of vegetal proteins is increasing rapidly in food applications due to their nutritional, environmental and economic benefits. However, their inclusion in food formulation implies adequate techno-functional properties, which mainly depends on the protein structure. Structure and technological properties of vegetal proteins are modified by the technological process applied during extraction (Stone et al., 2015, Fuhrmeister and Meuser, 2003), and conditioning (Sun and Arntfield, 2011, Ghribi et al., 2015, Shen and Tang, 2012). These processes may result in protein denaturation and/or aggregation (Shen and Tang, 2012).

Generally, globular proteins like whey proteins spontaneously and irreversibly aggregate when heated above 60 °C. The structure of globular protein aggregates formed after heating has been studied in detail (Nicolai and Durand, 2013). Earlier studies showed that in a first step, globular protein participates in a first aggregation or pre-aggregation leading to different structure depending on pH, ionic strength and concentration. Three distinctly morphologies of thermal aggregates have been observed: spherical particles (50 nm-few microns) next to the isoelectric point; strands (< 10 nm width, 10 nm – 10 µm length) far from the isoelectric point or with high net charge; and long semi-flexible fibrils (micron length) during heating at very low pH values (< 2.5) and low ionic strength (Nicolai and Durand, 2013). At higher protein concentration, these aggregates will re-aggregate in a secondary aggregation resulting in larger fractal clusters (Baussay et al., 2004, Mehalebi et al., 2008). Although the general features are common to most globular proteins, pea protein aggregates are widely unknown and need to be characterized for optimal functionality.

Structure and properties of protein aggregates are modified by technological process such as microfluidization. Microfluidization or dynamic high pressure modifies protein structure due to a combination of turbulence, shear and impact in a liquid by going through a fixed and small geometry. A previous study (Oliete et al., 2018) showed that microfluidization at 70 MPa and 130 MPa led to re-arrangements in the structure of pea globulin aggregates resulting in decreased protein particle size and hydrophobicity. Microfluidization at 120 MPa also resulted in modifications in physicochemical and conformational properties of soy protein aggregates that improved protein solubility and emulsifying ability (Shen and Tang, 2012). Dissanayake and Vasiljevic (2009) indicated that microfluidization at 140 MPa improved

solubility and emulsifying activity index of whey protein aggregates at pH 7 as a result of the disintegration of insoluble big aggregates into small soluble particles. In these studies, characterization and evaluation of the techno-functional properties of aggregated proteins were performed immediately after microfluidization. However, for industrial use, protein aggregates should follow at least a drying step to facilitate their conservation, transport and utilization.

Spray-drying and freeze-drying are the two most commonly used methods for drying proteins (Gong et al., 2016). Most of researchers in protein characterization use freeze-drying as a low temperature drying method to preserve the native structure of protein molecules, but the industrial production of food protein involves spray-drying because of the high cost and low productivity of freeze-drying. Differences in temperature and water evaporation process may affect differently protein structure and thus techno-functional properties of proteins (Tang et al., 2009, Mehalebi et al., 2008). The effect of drying method has been studied on the structure and technological properties of legume proteins such as soy protein (Hu et al., 2010), lentil (Joshi et al., 2011), rice dreg (Zhao et al., 2013), chickpea (Ghribi et al., 2015), peanut (Gong et al., 2016), and grass pea (Feyzi et al., 2018) proteins. Freeze-drying legume proteins showed more compact and ordered conformations (Zhao et al., 2013) with higher water/oil holding capacity and lower emulsifying and foaming properties than spray-dried proteins (Joshi et al., 2011, Hu et al., 2010, Ghribi et al., 2015, Gong et al., 2016, Zhao et al., 2013). Authors attributed differences between drying methods to lower protein denaturation during freeze-drying than during spray-drying. However, to our knowledge the effect of the drying method on the characteristics and functionality of plant protein aggregates has not been studied.

The aim of this work was to determine the effect of microfluidization and drying method (spray-drying vs freeze-drying) on some physicochemical characteristics of pea globulin aggregates accountable for their techno-functional properties. Globulin aggregates were characterized in terms of particle size, microstructure, charge, surface hydrophobicity and secondary structure of proteins. Protein solubility at different pH and suspension stability were also determined.

2. Material and Methods

2.1.Globulin extraction and proximate analysis

Pea flour, provided by Cosucra (Warcoing, Belgium), was a mixture of different cultivars. Flour was defatted by vigorous stirring in 5 volumes of petroleum ether for 1 h at room temperature (twice), and in 5 volumes of ethanol for 1 h at 4 °C (twice). The slurry was vacuum-filtered on a No. 2 porosity glass filter, and dried at room temperature for 48 h. Alkali extraction–isoelectric precipitation was used for globulin extraction as indicated by Mession et al. (2012). The dry flour was poured in a 0.1 M tris-HCl, pH 8 buffer and soluble proteins were extracted for 8 h at 4 °C (ratio flour-to buffer of 1:10). Insoluble materials were removed by centrifugation (10,000 *g*, 50 min, 20 °C). HCl 0.1 M was added to the supernatant up to pH 4.8 for globulin precipitation. Mixture was stirred for 1 h at 4 °C. Proteins were collected by centrifugation (10,000 *g*, 25 min, 4 °C), the pellets were washed with distilled water (pellet to water ratio of 1:25). The proteins were collected by centrifugation (10,000 *g*, 15 min, 4 °C), re-suspended at a concentration of 4 (w/w) and neutralized (pH 7.2) by adding slowly NaOH 0.25 M. The mixture was stirred at room temperature for 1 h, and again centrifuged to remove remaining insoluble material (10,000 *g*, 15 min, 4 °C). Globulins were frozen for 24 h at -18 °C and then freeze-dried in a Labconco Freeze dryer (Labconco, Kansas city, MO, USA). The process consisted in four steps of 24 h, at -50, -30, 0 and 25 °C. The resulting powder was stored at –18 °C until further use. The dry matter (95.38 ± 0.2% (w/w)) was determined according to AOAC International method 923.03 (AOAC, 1990). The protein content was 97.05% ± 0.2 (w/w) on a dry basis as determined by using the Kjeldahl method as AOAC International method 920.87 (AOAC, 1990) with a nitrogen conversion factor of 6.25 (Mession, Sok, Assifaoui, & Saurel, 2013, Shand, Ya, Pietrasik, & Wanasundara, 2007). The mineral content (2.36% ± 0.02 (w/w)) on a dry basis was determined as AOAC International method 945.39 (AOAC, 1990).

2.2.Preparation of aggregates

Pea protein aggregates were obtained using the protocol described by Chihi, Mession, Sok, & Saurel, (2016). 4% (w/w) globulin dispersions were prepared in 10 mM sodium phosphate buffer, pH 7.2, and stirred overnight at 4 °C to complete hydration. Sodium azide (0.05% w/w) was added as a preservative. The pH was adjusted to 7.2 with 0.1 M NaOH.

The dispersion was centrifuged at 10,000*g* for 20 min at 20 °C to remove insoluble proteins. The supernatant, with a protein concentration of 3.41% ± 0.04, was poured into tubes (0.5 cm in diameter) and placed in a temperature-controlled water bath previously equilibrated at 40

°C, then heated at 1 °C/min from 40 to 90 °C, incubated at 90 °C for 60 min, and rapidly cooled on ice for 10 min. Aggregated pea globulins showed no endothermic peak in the DSC thermogram (data not shown), indicative of complete protein denaturation due to thermal treatment.

Aggregated protein dispersions were subjected to microfluidization at 130 MPa (denoted as A130) in a LM10 Microfluidizer (Microfluidics, Newton, MA, USA) fitted with a Z-type chamber (G10Z). Samples were passed 3 times through the system. Aggregated protein samples without microfluidization treatment were denoted as A0. A0 and A130 samples were analyzed directly after preparation without drying.

2.3.Drying

Spray-drying or freeze-drying method was applied to microfluidized pea globulin aggregates (A130). For spray-drying (A130S) an atomizer Büchi Mini Spray Dryer B-290 (Büchi Sarl, Rungis, France) was used. The outlet temperature was fixed at 65 °C and the inlet temperature to 160 °C during drying. For freeze-drying (A130F) globulin solutions were first frozen for 24 h at -18 °C and then freeze-dried in a Labconco Freeze dryer (Labconco, Kansas city, MO, USA). Freeze-drying consisted in four steps of 24 h, at -50, -30, 0 and 25 °C.

After drying, aggregate samples were equilibrated at constant water activity of 0.293 ± 0.008% by storing for at least 7 days before analysis in a saturate ambient with potassium acetate. Water activity of aggregates was measured at least in triplicate with an Aqual Lab Dew Point Water Activity Meter 4TE (Aqua Lab, Pullman, WA, USA). Protein content of dried aggregates was 95.70% ± 0.44 for A130S and 95.42% ± 1.82 determined by the Kjeldahl method as indicated before.

2.4.Particle size

Size and distribution of pea globulin aggregates were measured using a laser diffraction particle size analyzer MasterSizer 3000 analyser (Malvern Instruments), with 10 mM phosphate buffer, pH 7.2, 0.05% (w/w) sodium azide as a dispersant. The relative refractive index of the dispersion was taken as 1.09, that is, the ratio of the refractive index of wheat gliadin considered as reference (1.45) to that of the continuous phase (1.33). All determinations were conducted at least in triplicate. Volume-average diameter, $d_{4,3}$ was reported as an indicative measure of particle size [Eq. 1]:

$d_{4,3} = \Sigma n_i d_i^4 / \Sigma n_i d_i^3$ [Eq. 1]

The particle size heterogeneity Span was calculated as [Eq. 2] :

$Span = [(d_{90} - d_{10}) / d_{50}]$ [Eq. 2]

2.5.Microscopy

Aggregated pea globulin suspensions were prepared in 10 mM phosphate buffer pH 7.2 for Transmission Electron Microscopy (TEM) by negative staining according to the procedure previously described by Munialo et al. (2014). A 10 µL aliquot of 125mg/mL aggregated pea globulin dispersions was deposited onto a carbon support film on a copper grid. The excess was removed after 30 min using a filter paper (Whatman no. 1, 512-1002, VWR International Europe BVBA, Leuven, Belgium). A droplet of 3% uranyl acetate at pH 3.8 was added for 30 s to improve the contrast. Excess uranyl acetate was removed by use of a filter paper. Electron micrographs were obtained using a Hitachi H-7500 transmission electron microscope (Hitachi High-Technologies Europe GmbH) equipped with an AMT camera driven by AMT software (Hitachi) operating at 80 kV.

2.6.Fourier transform infrared (FTIR) spectroscopy

The secondary structure of aggregated pea proteins was characterized using FTIR spectroscopy. Aggregated pea protein suspensions (A0 and A130) were poured in a crystallizer forming a thin layer, dehydrated at 40 °C until water elimination and manually ground. A130S and A130F were analyzed as they were. FTIR spectra were collected in the wave number range from 600 to 4000 cm^{-1} with a resolution of 4 cm^{-1} using a Spectrum 65 FT-IR spectrometer (Perkin-Elmer, Courtaboeuf, France). The spectra were the average of 32 scans.

2.7.Zeta potential

The electrical charge (ζ-potential) of aggregates was measured using a ZetaCompact Z8000 zetaphoremeter (CAD Instruments, Les Essarts, Le Roi, France). The samples were diluted with 10 mM phosphate buffer, pH 7.2, to about 25 µg/g to obtain a tracking value of at least 100. The temperature of the cell was maintained at ambient temperature. The data was the average value of at least 5 measurements.

2.8.Surface hydrophobicity

Protein surface hydrophobicity (H_o) was determined with the fluorescence probe 1-anilinonaphthalene-8-sulfonic acid (ANS; Sigma, St. Louis, MO, USA), according to the method of Kato and Nakai (1980) modified by Karaca et al. (2011). Aggregates were diluted in a range of concentrations from 0.004% to 0.02% (w/w) in 10 mM phosphate buffer pH 7.2. 20 μL of the 8 mM ANS solution prepared in the same buffer were added to 4 mL of each protein sample, and the mixture was kept in the dark for 15 min. To ensure sufficient ANS to link the free surface hydrophobic groups of the protein, a calibration curve was constructed with the most concentrated protein solution (0.02%). The fluorescence intensity was measured using an LS-50B luminescence spectrometer (PerkinElmer, Waltham, MA, USA) at 380 nm (excitation) and 460 nm (emission). Blanks were protein samples without ANS and buffer with ANS. The initial slope of the fluorescence intensity versus protein concentration (mg/mL) plot, calculated by linear regression analysis, was used as an index of protein surface hydrophobicity.

2.9.Solubility

1% (w/w) aggregated pea globulin suspensions were hydrated overnight in 10 mM phosphate buffer at pH 3 to 8 at 4 °C. Subsequently, the suspensions were centrifuged at 10000 *g* for 20 min at 4 °C. The protein content in the supernatant was determined by Kjeldhal method. Protein solubility was determined as Nitrogen Solubility Index (NSI) by dividing the nitrogen content of the supernatant by the total nitrogen in the sample (x100%). Analyses were performed in triplicate.

2.10. Suspension Stability

The stability of 5% (w/w) aggregated globulin suspensions in 10 mM phosphate buffer pH 7.2 was measured by Turbiscan® Lab Expert (Formulaction, Toulouse, France). Turbiscan® measurements are based in multiple light scattering. The equipment possesses two optical sensors that measure the transmitted and the backscattered near-infrared monochromatic light (λ = 800nm). Mengual, Meunier, Cayre, Puech, & Snabre (1999) indicated the ability of this technique to characterize particle or aggregate size variation and particle/aggregate migration. In diluted systems (transmission variation > 0.2%), these phenomena are measured by the transmission light intensity of the sample as a function of sample height and time. The measurement of the backscattering light in non-opaque systems can give erroneous information since the backscattering profiles can be affected by the partial reflection of the light crossing the sample. Suspensions were maintained under agitation until analysis.

Samples were placed in flat-bottomed cylindrical borosilicate glass tubes and introduced into Turbiscan® measurement cell. Turbiscan detection head scanned the sample by moving vertically along the analysis cell and acquiring data every 40 µm. The light scattering profiles were recorded every 10 minutes for 12 hours. Differences in the transmission profiles along time indicate sample instability. Light transmitted intensity (T) is affected by the average diameter of particles and the mean free-path of photon. T may change over time and height. Light transmitted intensity (T) Based on Turbiscan® graphs three different regions were distinguished along the tube axis: the bottom, the middle and the top. Variations of T in the top and in the bottom of the sample are related to migration phenomena, such as clarification (top) and sedimentation (bottom). The variations of T in the middle part of the sample indicate the interaction phenomena between particles, and thus particle size variation. Based on the obtained spectra, suspension stability can be calculated by Turbiscan stability index (TSI) according to equation Eq.3

$$TSI = \sum_i \frac{\sum_h |Scan_i(h) - Scan_{i-1}(h)|}{H} \qquad \text{[Eq.3]}$$

Where H: sample height from bottom of the cell to the meniscus

$Scan_i(h)$: intensity of scanning light (time is i, height is h)

$Scan_{i-1}(h)$: intensity of scanning light (time is i-1, height is h)

The lowest TSI values indicated the most stable suspensions. Turbiscan® spectra were analyzed with the software Turbisoft-Lab version 2.2.0.82-5 (Formulaction, Toulouse, France).

2.11. Statistical analysis

Differences between samples (A0, A130, A130S, A130F) were studied by analysis of variance (one-way ANOVA). Significance was set at $p < 0.05$. Tukey's post-hoc least-significant-differences method was used to describe means with 95% confidence intervals. The statistical analyses were performed using Statistica software, version 12 (Tulsa, OK, USA).

3. Results

3.1. Particle size

The particle size distribution of pea globulin aggregates obtained by laser granulometry at pH 7.2 was displayed in Figure 1. Particle size distribution of pea aggregate samples before microfluidization and drying (A0) showed a high peak around 600 nm that corresponded to

the highest volume fraction of aggregates. Another heterogenic population with particle size ranging from ~4 to ~200 µm was observed and corresponded to highly aggregated pea globulins. When microfluidization at 130 MPa was applied (A130) particle size distribution shifted to smaller values compared to A0 (Figure 1), decreasing the volume-average diameter and the distribution heterogeneity (Table 1). Drying microfluidized pea globulin aggregates (A130S, A130F) caused the drastic reduction of the smallest-sized population and formed big-sized aggregates (1 – 100 µm) (Figure 1). Freeze-drying (A130F) showed higher $d_{4,3}$ values compared to A130S (Table 1).

Figure 1.

Table 1.

3.2. Microscopy

Figure 2 presented transmission electron micrographs (TEM) of pea globulin aggregates at pH 7.2. Pea globulin aggregates before microfluidisation and drying (A0) appeared as small curved strands, which agglomerated and formed secondary aggregates (Figure 2a). After microfluidization at 130 MPa (A130), secondary aggregates disappeared and primary aggregates showed smaller and more angular-shaped than in A0 (Figure 2b). Drying after microfluidization (A130S, A130F) favored the formation of voluminous secondary aggregates compared to A130, especially when freeze-drying (A130F) was used compared to spray-drying (A130S) (Figure 2 c and d respectively).

Figure 2.

3.3.FTIR spectra analysis

Figure 3 showed the amide I region (1700 – 1600 cm^{-1}) of pea protein aggregates, permitting to identify the characteristic bands of the protein secondary structure. Amide I region mainly comprises the stretching vibration of C=O (Ellepola, Choi, and Ma, 2005). The obtained bands were assigned to different conformations according to existing data (Yang, Liu, Zeng, and Chen, 2018, Gharsallaoui et al., 2012) as indicated in Table 2. Microfluidization at 130 MPa (A130) decreased the intensity of peaks 1602 cm^{-1} (corresponding to vibration of amino acid residues), 1614 cm^{-1} (corresponding to antiparallel β-sheet), 1634 cm^{-1}, 1641 cm^{-1}

(corresponding to β-sheet) and 1694 cm^{-1} (corresponding to aggregated strands), compared to A0, whereas it increased the intensity of peaks 1668 cm^{-1} and 1681 cm^{-1} (corresponding to β-turn). Drying microfluidized pea aggregates by spray-drying (A130S) markedly increased the intensity of peak 1652 cm^{-1} (corresponding to random coil), 1683 cm^{-1} (corresponding to β-turn), and 1695 cm^{-1} (corresponding to aggregated strands) compared to A130. In parallel, freeze-drying slightly increased the intensity of peaks 1630 cm^{-1} and 1638 cm^{-1} (corresponding to β-sheet), and reduced the intensity of peaks 1646 cm^{-1} (corresponding to random coil), and 1662 cm^{-1} and 1684 cm^{-1} (corresponding to β-turn).

Figure 3 and Table 2

3.4. Surface hydrophobicity and ζ-potential

The surface hydrophobicity (H_o) of aggregates at pH 7.2 was evaluated using an ANS fluorescence probe (Table 1). Pea globulin aggregates before microfluidization and drying (A0) showed the highest H_o values. Microfluidization at 130 MPa (A130) significantly decreased surface hydrophobicity of pea globulin aggregates (~6% reduction). Drying after microfluidization (A130S, A130F) notably decreased H_o (~30% reduction), but no significant differences were observed between freeze- (A130F) and spray-drying (A130S) methods.

No significant differences were observed in the charge (ζ-potential) of pea globulin aggregates due to the technological process i.e. microfluidization and drying (Table 1).

3.5.Protein Solubility

The solubility profile of pea globulin aggregates as a function of pH (Figure 4) showed an inverted bell shape with the minimum around pH 5 which is near the isoelectric point (pI) of globulins. Microfluidization at 130 MPa did not significantly improved solubility of pea globulin aggregates compared to A0. Drying microfluidized aggregates (A130S, A130F) notably reduced solubility of microfluidized pea globulin aggregates except at pH 5. Comparing drying methods, no significant differences were observed between freeze-dried samples (A130F) and spray-dried samples (A130S).

Figure 4.

3.6.Suspension stability

Figure 5 showed the transmission profiles of pea aggregates obtained by Turbiscan® in delta mode, i.e. the first scan was subtracted from all other scans during time, which allowed easier visualization of the transmission flux variations (Cvek, Mrlik, Moucka, and Sedlacik, 2018).

A0 samples showed a stable transmission profile (Figure 5a). The decrease of transmission in the bottom of the sample indicating modest sedimentation of particles in suspension would be negligible since transmission variation did not reach 2%. In A130 samples, T noticeably increased in the top of A130 sample (Figure 5b) indicating the formation of a clarification layer. The increase in the middle of the sample indicated that particles increased in size (flocculation) allowing photons to go through the sample without being diffused.

Drying of microfluidized pea globulin aggregates (A130S, A130F) induced less transmission flux variation than A130 samples (Figure 5c and d respectively). A130S formed a limited clarification layer at the top of the sample (Figure 5c). A130F formed a clarification layer similar to A130 but the increase in particle size (transmission increase in the middle of the sample) was smaller (Figure 5d).

Figure 5.

Figure 6 permitted the analysis of the global stability by means of TSI variation. A0 showed the smallest TSI variation in accordance with the most stable transmission profile. A130 showed the highest TSI values as a result of the clarification and flocculation phenomena that took place during measurements. Instability in A130 was especially intense during the first five hours as indicated the notable TSI variation. Drying decreased the instability of samples compared to A130, especially in A130S.

Figure 6.

4. Discussion

Microfluidization effect on pea globulin aggregates characteristics

Pea globulin aggregates before microfluidization and drying (A0) appeared as small curved strands in the micrographs obtained by TEM, as already indicated by Nicolai et al. (2011) and Jung et al. (2008) for β-lactoglobulin aggregates at neutral pH. Primary aggregates agglomerated into secondary aggregates as fractal clusters in which a self-similar structure

was repeated (Baussay et al., 2004, Mehalebi et al., 2008). β-sheet were the dominant secondary structure in A0 as revealed the strong absorption at 1640 cm^{-1} in the amine I region, confirming previous results concerning legume globulins: soy protein thermal aggregates (Zhang, Liang, Tian, Chen, and Subirade, 2012), faba bean protein isolate (Yang et al., 2018), and field pea and kidney bean globulins (Shevkani, Singh, Kaur, and Rana, 2015). The negative charge obtained in all pea aggregate samples was related to the working pH value (pH 7.2) which is higher than pI of vicilins (pI 4.5, Ezpeleta et al., 1996) and pI of legumin acid subunit (pI 4.7, Krishina et al., 1979). At pH 7.2, amine and carboxylic free groups of proteins are deprotonated. Charge values were included in the range between -10 and -15mV defined by Riddick (1968) as aggregation threshold, which is in agreement with the observation of protein aggregation.

Microfluidization at 130 MPa modified the structure of pea globulin aggregates as clearly observed by TEM, FTIR, and particle size distribution. The combination of turbulence, shear and collisions caused by microfluidization at 130 MPa broke secondary aggregates and modified the conformation of primary aggregates which appeared smaller, more homogeneous in size and more angular in shape than in A0. Small sized aggregates obtained by microfluidization (compared to initially present aggregates) underwent structural re-arrangement. Microfluidization seemed to induce the unfolding of β-sheet structures producing a self-reassembly to less ordered structures as β-turns, while most of the other secondary structures of pea protein aggregates were almost maintained. Yang et al. (2018) also indicated that high pressure homogenization at 207 MPa had a certain impact on faba bean protein, but most of the secondary structures were intact. These authors however observed a decrease of α-helix and β-turn after homogenization. Wang, Li, Jiang, Qi and Zhou, (2014) signaled that the processing conditions such as temperature and time determine the protein secondary structures of soybean proteins. New re-arrangements hided hydrophobic groups, made them less accessible to the binding of ANS fluorescence probe, and resulted in decrease of surface hydrophobicity (Oliete et al., 2018). However, Shen and Tang (2012) observed an increase in hydrophobicity after 120 MPa microfluidization of soy aggregates applied after a 30 min thermal treatment. Hydrophobicity behavior of aggregates was clearly dependent on the temperature and time used in the thermal aggregation (Shen and Tang, 2012, Wang et al., 2014). The charge of pea globulin aggregates was not significantly modified by microfluidization as already indicated in previous works (Oliete et al., 2018). The absence of significant differences in the ζ-potential within samples could be related to the presence of

salts coming from the extraction method (~2.4% mineral content in the dried protein isolate). Salt could surround the protein, reducing the ζ- potential absolute value by screening effect and thus the amount of electrostatic repulsive forces (Lam et al., 2018).

Structural changes induced by microfluidization at 130 MPa did not reach to significantly improve solubility of pea globulin aggregates. Solubility is an important prerequisite for proteins to be used in food applications, since it affects all other techno-functional properties. Dissanayake and Vasiljevic (2009) and Shen and Tang (2012) indicated that microfluidization of whey and soy aggregates increased solubility, as a result of several complementary factors. First of all, high shearing due to microfluidization will disrupt large insoluble aggregates into small soluble ones (Shen and Tang, 2012), and size reduction would decrease sedimentability of particles (Meerdink and Van't Riet, 1995). In the case of pea globulin aggregates, microfluidization at 130 MPa decreased the volume-average diameter of particles. However, the non-negligible residual big sized particles in A130 would hinder the increase of solubility caused by the increased in submicron sized particles. These big sized particles (>10 μm) could come from the non-microfluidized sample or could be formed after microfluidization. New arrangements resulting in less ordered secondary structure could favour interactions between particles. Secondly, protein solubility depends on the protein-water interactions which are driven mainly by the protein surface charge and the presence of free hydrophobic groups, at pH values far from the pI. Since no difference in particle charge was observed between A0 and A130, we rather suggest that hydrophobic attractive interactions play a predominant role regarding hydration properties of protein aggregates. In fact, Karaca et al. (2011) observed a negative correlation between protein solubility and surface hydrophobicity. Lower surface hydrophobicity made microfluidized aggregates less compact and more flexible (Tang et al., 2009) than non-microfluidized aggregates. Lower aggregate compactness would facilitate the interactions between proteins and water molecules (Feyzi et al., 2018). In the present case, similar solubility values between microfluidized and non-microfluidized pea globulin aggregates indicated that, despite significant difference in hydrophobicity, the presence of big sized particles would define the solubility behavior of pea globulin aggregates. Microfluidization at 130 MPa was in detrimental to suspension stability as revealed by enhanced flocculation and clarification phenomena during Turbiscan® test . New re-arrangements induced by microfluidization would favour protein-protein interactions, resulting in increasing particle size along time, which was not measurable by laser diffraction due to highly diluted sample conditions. These interactions were probably driven by hydrogen

bonds. Electrostatic interactions are managed by particle charge which did not significantly vary between samples in the present work. Hydrophobic interactions decreased between A0 and A130 as was indicated by the significant reduction of surface hydrophobicity measured by fluorescence probing.

Drying effects on microfluidized pea globulin aggregates characteristics

Drying after microfluidization (A130F, A130S) caused the re-aggregation of pea globulin proteins, as indicated by the particle size data and the TEM observations. Drying increased connection points between primary aggregates leading to branched fractal objects. These effects were more noticeable when freeze-drying (A130F) was used compared to spray-drying (A130S). Other authors (Cepeda et al., 1998; Ghribi et al., 2015; Joshi et al., 2011; Zhao et al., 2013) already indicated that freeze-dried protein showed higher particle size than other more intense drying methods such as spray-drying or hot air convection. In the case of freeze-drying, local cryo-concentration during freezing would increase opportunities of aggregated proteins to come into close contact with one another. In consequence freeze-drying would favour molecular interactions such as electrostatic interactions, hydrophobic interactions and even disulfide bridges (Gong et al., 2016) resulting in compact protein conformations (Zhao et al., 2013). On the other hand, spray-drying process forces the sample through a nozzle forming small droplets that encounter dry and hot air. The drastic kinetics conditions of spray-drying process compared to freeze-drying may limit interactions between molecules and make aggregation more difficult. Differences between drying methods have been observed even in the secondary structure of pea proteins as other authors (Feyzi et al., 2018; Lan, Xu, Ohm, Chen and Rao, 2018). Peaks in the amide I region from dried samples shifted compared to peaks of non-dried samples, suggesting that the protein structures were affected by the drying methods (Zhao et al., 2013). Freeze-drying (A130F) seemed to increase the β-sheet structure and decreased the random coils and β-turns. Spray-drying (A130S) markedly increased random coils which became the predominant structure, β-turns and aggregated strandsindicating significant conformation changes to less ordered secondary structure. Simultaneously, the drying method did not show a clear effect on H_o. Similar values of Ho for A130S and 130F samples were indeed observed despite different effects of the drying method on secondary structure of proteins. Thus, new arrangements between molecules in protein aggregates induced by dehydration (A130S, A130F), tended to bury polypeptides with hydrophobic groups which were initially exposed in non-dried microfluidized pea globulin aggregates, decreasing surface hydrophobicity. Whilst Zhao et al. (2013) signaled higher

surface hydrophobicity in spray-drying rice dreg protein isolate compared to freeze-dried, Gong et al. (2016) observed higher H_o values in freeze-dried peanut isolate than in spray-dried one. Feyzi et al. (2018) signaled different effect of drying method on H_o depending on the protein extraction method used.

Changes in the structure of microfluidized pea globulin aggregates caused by drying decreased protein solubility but improved suspension stability, compared to their non-dried counterpart. The decrease in solubility of dried microfluidized pea globulin aggregates was related to higher particle size and thus higher sedimentability of rehydrated aggregates (A130S, A130F) compared to non-dried microfluidized aggregates (A130). The negative effect of increasing particle size due to drying on protein solubility seemed to prevail over the positive effect caused by the decrease of the surface hydrophobicity resulting from re-aggregation. This statement was already suggested above to explain the effect of microfluidization on pea globulin aggregate solubility. The effect of particle size on pea globulin solubility behavior overcomes the effect caused by re-arrangement in aggregate structure modification. Comparing drying methods, freeze-drying (A130F) and spray-drying (A130S) did not show significant differences in solubility. Contradictory results have been published about the effect of the drying method on protein solubility. Hu et al. (2010) and Sumner et al. (1981) reported that spray-dried soy and pea proteins had lower solubility compared to the freeze-dried counterparts. However, Cepeda et al. (1998), Johsi et al. (2011), and Zhao et al. (2013) reported that the solubility of spray-dried faba bean, soy and rice dreg proteins respectively was higher than that of freeze-dried samples. In the case of microfluidized pea globulin aggregates, the presence of big sized particles in both spray- and freeze-dried aggregates would determine their solubility behavior. Drying A130S and A130F improved suspension stability compared to A130. Protein re-aggregation caused by drying would create a stable structure with limited particle size evolution, probably due to enhanced steric repulsion. Increase in protein particle interactions in A130S and A130F was hindered compared to A130, and led to a reduction of the clarification effect. Freeze-dried microfluidized pea globulin aggregates (A130F) showed lower suspension stability than A130S which was in accordance with higher initial particle size.

5. Conclusion

In the current study, the effect of microfluidization and drying method on the structure, solubility and suspension stability of pea globulin aggregates were investigated.

Microfluidization at 130 MPa broke pea globulin aggregates and formed smaller, more angular-shaped, and lower surface-hydrophobicity particles with less ordered protein structure compared to pea globulin aggregates before microfluidization. Solubility of pea globulin aggregates seemed to be defined by particle size more than protein structure. However, the new re-arrangements produced by microfluidization led to less suspension stability due to time-evolving flocculation. Drying microfluidized aggregates favored re-aggregation of particles with modifications in structural conformation of proteins, and significantly decreased surface hydrophobicity. The new structures created in dried microfluidized pea globulin aggregates decreased solubility but increased suspension stability. Comparing drying methods spray-dried aggregates showed lower re-aggregation than freeze-dried aggregates, resulting in smaller particle size what improved suspension stability. This study showed that drying methods determine the structure of microfluidized pea globulin aggregates and will impact their techno-functional properties. These findings are decisive for using pea globulin aggregates as dry powders in the preparation of suspensions, emulsions and gels for the food industry.

Funding: This work was supported financially by European Funds for Regional Development (FEDER-FSE Bourgogne 2014/2020), French Inter-Ministerial Unique Funds (FUI), and the Region of Burgundy (France) as part of project LEGUP Lot 3 2015 03 03.

Acknowledges: Authors would thank the Centre de Microscopie INRA/uB (Dijon) of the Plateforme DImaCell Platform (INRA, Univ. Bourgogne Franche-Comté, F-21000 Dijon, France. Authors would also thank Formulaction company.

6. References

AOAC. Association of Official Analytical Chemists International. (1990). *Official methods of analysis*. (15th ed.). Arlington, VA: Association of Official Analytical Chemists, Inc.

Baussay, K., Le Bon, C., Nicolai, T., Durand, D., & Busnel, J. P. (2004). Influence of the ionic strength on the heat-induced aggregation of the globular protein β-lactoglobulin at pH7. *International Journal of Biological Macromolecules*, 34, 21 – 28.

Cepeda, E., Villaran, M.C., & Aranguiz, N. (1998) Functional properties of faba bean (*Vicia faba*) protein flour dried by spray drying and freeze drying. *Journal of Food Engineering*, 36, 303 – 310.

Chihi, M., Mession, J. L., Sok, N., & Saurel, R. (2016). Heat-induced soluble protein aggregates from mixed pea globulins and β-lactoglobulin. *Journal of Agricultural and Food Chemistry*, 64, 2780 – 2791.

Cvek, M., Mrlik, M., Moucka, R., & Sedlacik, M. (2018). A systematical study of the overall influence of carbon allotrope additives on performance, stability and redispeersibility of magnetorheological fluids. *Colloids and Surfaces A*, 543, 83 – 92.

Dissanayake, M., & Vasiljevic, T. (2009). Functional properties of whey proteins affected by heat treatment and hydrodynamic high-pressure shearing. *Journal of Dairy Science*, 92, 1387 – 1397.

Ellepola, S. W., Choi, S. M., & Ma, C. Y. (2005). Conformational study of globulin from rice (*Oryza sativa*) seeds by Fourier-transform infrared spectroscopy. *International Journal of Biological macromolecules*, 37, 12 – 20.

Ezpeleta, I., Irache, J. M., Stainmesse, S., Gueguen, J., & Orecchioni, A. M. (1996). Preparation of small-sized particles from vicilin (vegetal protein from *Pisum sativum* L.) by coacervation. *European Journal of Pharmaceutics and Biopharmaceutics*, 42, 36 – 41.

Feyzi, S., Milani, E., & Golimovahhed, Q. A. (2018). Grass pea (*Lathyrus sativus* L.) protein isolate: the effect of extraction optimization and drying methods on the structure and functional properties. *Food Hydrocolloids*, 74, 187 – 196.

Fuhrmeister, N. H., & Meuser, F. (2003). Impact of processing on functional properties of protein products from wrinkled peas. *Journal of Food Engineering*, 56, 119 – 129.

Gharsallaoui, A., Roudaut, G., Beney, L., Chambin, O., Voilley, A., & Saurel, R. (2012). Properties of spray-dried food flavours microencapsulated zith two-layered membranes: Roles of interfacial interactions and water. Food Chemistry, 132, 1713 – 1720.

Ghribi, A. M., Gafsi, I. M., Blecker, C., Danthine, S., Attia, H., & Besbes, S. (2015). Effect of drying methods on physico-chemical and functional properties of chickpea protein concentrates. *Journal of Food Engineering*, 165, 179 – 188.

Gong, K. J., Si, A. M., Liu, H. Z., Liu, L., Hu, H., Adhikari, B., & Wang, Q. (2016). Emulsifying properties and structure changes of spray and freeze-dried peanut protein isolate. *Journal of Food Engineering*, 170, 33 – 40.

Hu, X., Cheng, Y., Fan, J., Lu, Z., Yamaki, K., & Li, L. (2010) Effects of drying methods on physicochemical and functional properties of soy protein isolates. *Journal of Food Process Preservation*, 34, 520 – 540.

563 Joshi, M., Adhikari, B., Aldred, P., Panozzo, J.F., & Kasapis, S. (2011). Physicochemical and
564 functional properties of lentil protein isolates prepared by different drying methods. *Food*
565 *Chemistry*, 129, 1513 – 1522.
566 Jung, J. M., Savin, G., Pouzot, M., Schmitt, C., & Mezzenga, R. (2008). Structure of heat-
567 induced β-lactoglobulin aggregates and their complexes with sodium-dodecyl sulfate.
568 *Biomacromolecules*, 9, 2477 – 2486.
569 Karaca, A. C., Low, N., & Nickerson, M. (2011). Emulsifying properties of chickpea, faba
570 bean, lentil and pea proteins produced by isoelectric precipitation and salt extraction. *Food*
571 *Research International*, 44, 2742 – 2750.
572 Kato, A., & Nakai, S. (1980). Hydrophobicity determined by a fluorescence probe method
573 and its correlation with surface properties of proteins. *Biochimica et Biophysica Acta*, 624, 13
574 – 20.
575 Krishina, T. G., Croy, R. R. D., & Boulter, D. (1979). Heterogeneity in subunit composition
576 of the legumin of *Pisum sativum*. *Phytochemistry*, 18, 1879 – 1880.
577 Lam, A. C. Y., Tyler, R. T., & Nickerson, M. T. (2018). Pea protein isolates: structure,
578 extraction and functionality. *Food Reviews International*, 34, 126 – 147.
579 Lan, Y., Xu, M., Ohm, J. B., Chen, B., & Rao, J. (2018). Solid dispersion-based spray-drying
580 improves solubility and mitigates beany flavor of pea protein isolae. *Food Chemistry*,
581 https://doi.org/10.1016/j.foodchem.2018.11.074.
582 Meerdink, G., & Van't Riet, K. (1995) Modeling segregation of solute material during drying
583 of liquid foods. *AIChE Journal*, 41, 732 – 736.
584 Mehalebi, S., Nicolai, T., & Durand, D. (2008). Light scattering study of heat-denatured
585 globular protein aggregates. *International Journal of Biological Macromolecules*, 43, 129 –
586 135.
587 Mengual, O., Meunier, G., Cayre, I., Puech, K., & Snabre, P. (1999). Characterisation of
588 instability of concentrated dispersions by a new optical analyser: The TURBISCAN MA
589 1000. *Colloids and Surfaces A*, 152, 111 – 123.
590 Mession, J. L., Assifaoui, A., Cayot, P., & Saurel, R. (2012). Effect of pea proteins extraction
591 and vicilin/legumin fractionation on the phase behaviour in admixture with alginate. *Food*
592 *Hydrocolloids*, 29, 335 – 346.
593 Mession, J. L., Sok, N., Assifaoui, A., & Saurel, R. (2013). Thermal denaturation of pea
594 globulins (*Pisum sativum* L.)—molecular interactions leading to heat-induced protein
595 aggregation. *Journal of Agricultural and Food Chemistry*, 61, 1196 – 1204.

Munialo, C. D., Martin, Q. H., van der Linden, E., & de Jongh H.H.J. (2014). Fibril Formation from Pea Protein and Subsequent Gel Formation. *Journal of Agriculture and Food Chemistry*, 62, 2418 – 2427.

Nicolai, T., & Durand, D. (2013). Controlled food protein aggregation for new functionality. *Current Opinion in Colloid and Interface Science*, 18, 249 – 256.

Nicolai, T., Britten, M., & Schmitt, C. (2011). beta-lactoglobulin and WPI aggregates: formation, structure and applications. *Food Hydrocolloids*, 25, 1945 – 1962.

Oliete, B., Potin, F., Cases, E., & Saurel, R. (2018). Modulation of the emulsifying properties of pea globulin soluble aggregates by dynamic high-pressure fluidization. *Innovative Food Science and Emerging Technologies*, 47, 292 – 300.

Qi, P. X.,Ren, D., Xiao, Y., & Tomasula, M. (2015). Effect of homogenization and pasteurization on the structure and stability of whey protein in milk. *Journal of Dairy Science*, 98, 2884 - 2897.

Riddick, T. M. (1968). *Control of colloid stability through zeta potential*. Wynnewood, PA: Livingston Publishing Company.

Shand, P. J., Ya, H., Pietrasik, Z., & Wanasundara, P. K. J. P. K. (2007). Physicochemical and textural properties of heat-induced pea protein isolate gels. *Food Chemistry*, 102, 1119 – 1130.

Shen, L., & Tang, C. H. (2012). Microfluidization as a potential technique to modify surface properties of soy protein isolate. *Food Research International*, 48, 108 – 118.

Shevkani, K., Singh, N., Kaur, A., & Rana, J. C. (2015). Structural and functional characterization of kidney bean and field pea protein isolates: A comparative study. *Food Hydrocolloids*, 43, 679 – 689.

Stone, A. K., Karalash, A., Tyler, R. T., Zarkentin, T. D., & Nickerson, M. T. (2015). Functional attributes of pea protein isolates prepared using different extraction methods and cultivars. *Food Research International*, 76, 31 – 38.

Sumner, A. K., Nielsen, M. A., & Youngs, C. G. (1981). Production and evaluation of pea protein isolate. *Journal of Food Science*, 46, 364 – 372.

Sun, X. D., & Arntfield, S. D. (2011). Gelation properties of salt-extracted pea protein isolate induced by heat treatment: Effect of heating and cooling rate. *Food Chemistry*, 124, 1011 – 1016.

Tang, C. H., Sun, X., & Yin, S. W. (2009). Physicochemical, functional and structural properties of vicilin-rich protein isolates from three *Phaseolus* legumes: Effect of heat treatment. *Food Hydrocolloids*, 23, 1771 – 1778.

630 Wang, Z., Li, Y., Jiang,L., Qi, B., & Zhou, L. (2014). Relationship between secondary
631 structure and surface hydrophobicity of soybean protein isolate subjected to heat treatment.
632 *Journal of Chemistry*, http://dx.doi.org/10.1155/2014/475389.
633 Yang, J., Liu, G., Zeng, H., & Chen, L. (2018). Effects of high pressure homogenization on
634 faba bean protein aggregation in relation to solubility and interfacial properties. *Food*
635 *Hydrocolloids*, 83, 275 – 286.
636 Zhang, J., Liang, L., Tian, Z., Chen, L., & Subirade, M. (2012). Preparation and in vitro
637 evaluation of calcium-induced soy protein isolate nanoparticles and their formation
638 mechanism study. *Food Chemistry*, 133, 390 – 399.
639 Zhao, Q., Xiong, H., Selomulya, C., Chen, X. D., Huang, S., Ruan, X., Zhou, Q., & Sun, W.
640 (2013). Effects of spray drying and freeze drying on the properties of protein isolate from rice
641 dreg protein. *Food Bioprocess Technology*, 6, 1759 – 1769.

Figure captions

Figure 1. Particle size distribution profiles of pea globulin aggregates before microfluidization and drying (A0), after microfluidization at 130 MPa (A130), and after microfluidization and spray-drying (A130S) or freeze-drying (A130F) in 10 mM phosphate buffer at pH 7.2.

Figure 2. Transmission electron micrographs (TEM) of pea globulin aggregates pea globulin aggregates before microfluidization and drying (A0) (a), after microfluidization at 130 MPa (A130) (b), and after microfluidization and spray-drying (A130S) (c) or freeze-drying (A130F) (d) in 10 mM phosphate buffer at pH 7.2.

Figure 3. Deconvoluted FTIR spectra in the amine I region of pea globulin aggregates before microfluidization and drying (A0), after microfluidization at 130 MPa (A130), and after microfluidization and spray-drying (A130S) or freeze-drying (A130F).

Figure 4. Nitrogen Solubility Index (%) of pea globulin aggregates before microfluidization and drying (A0), after microfluidization at 130 MPa (A130), and after microfluidization and spray-drying (A130S) or freeze-drying (A130F).

Figure 5. Turbiscan® spectra of pea globulin aggregates before microfluidization and drying (A0), after microfluidization at 130 MPa (A130), and after microfluidization and spray-drying (A130S) or freeze-drying (A130F) in 10 mM phosphate buffer at pH 7.2.

Figure 6. Turbiscan Stability Index (TSI) variation of pea globulin aggregates before microfluidization and drying (A0), after microfluidization at 130 MPa (A130), and after microfluidization and spray-drying (A130S) or freeze-drying (A130F) in 10 mM phosphate buffer at pH 7.2.

Figure 1.

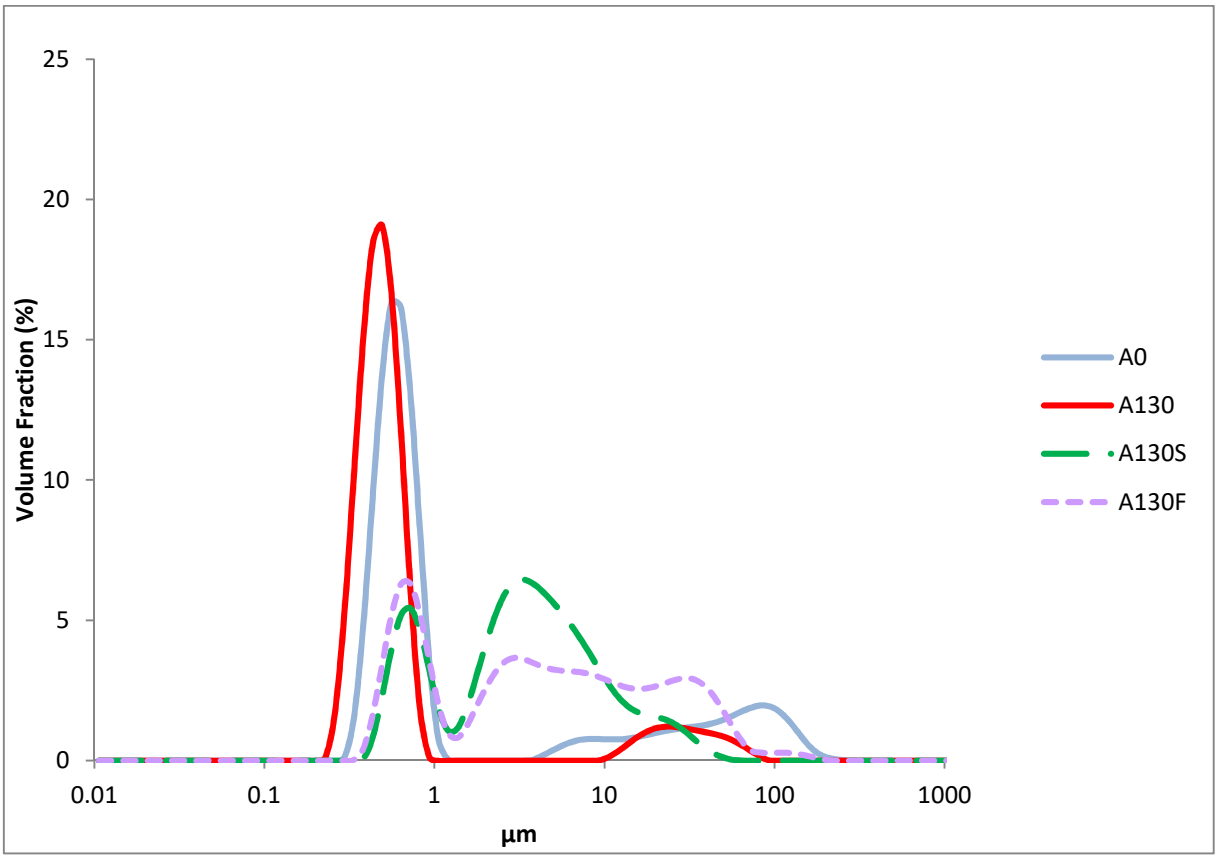
25
20
15
10
5
0
Volume Fraction (%)
0.01
0.1
1
10
100
1000
µm
A0
A130
A130S
A130F

Figure 2.

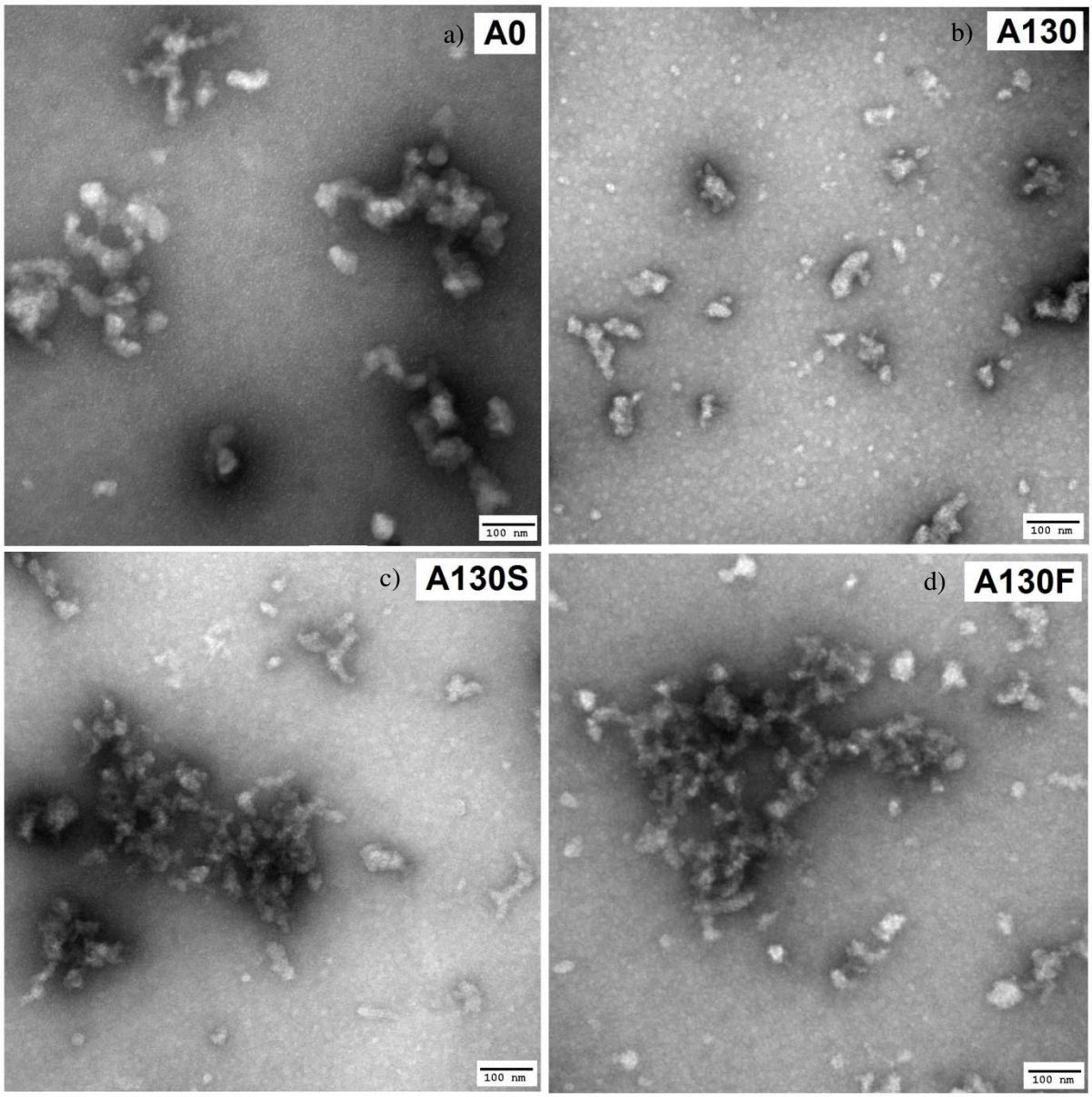

Figure 3

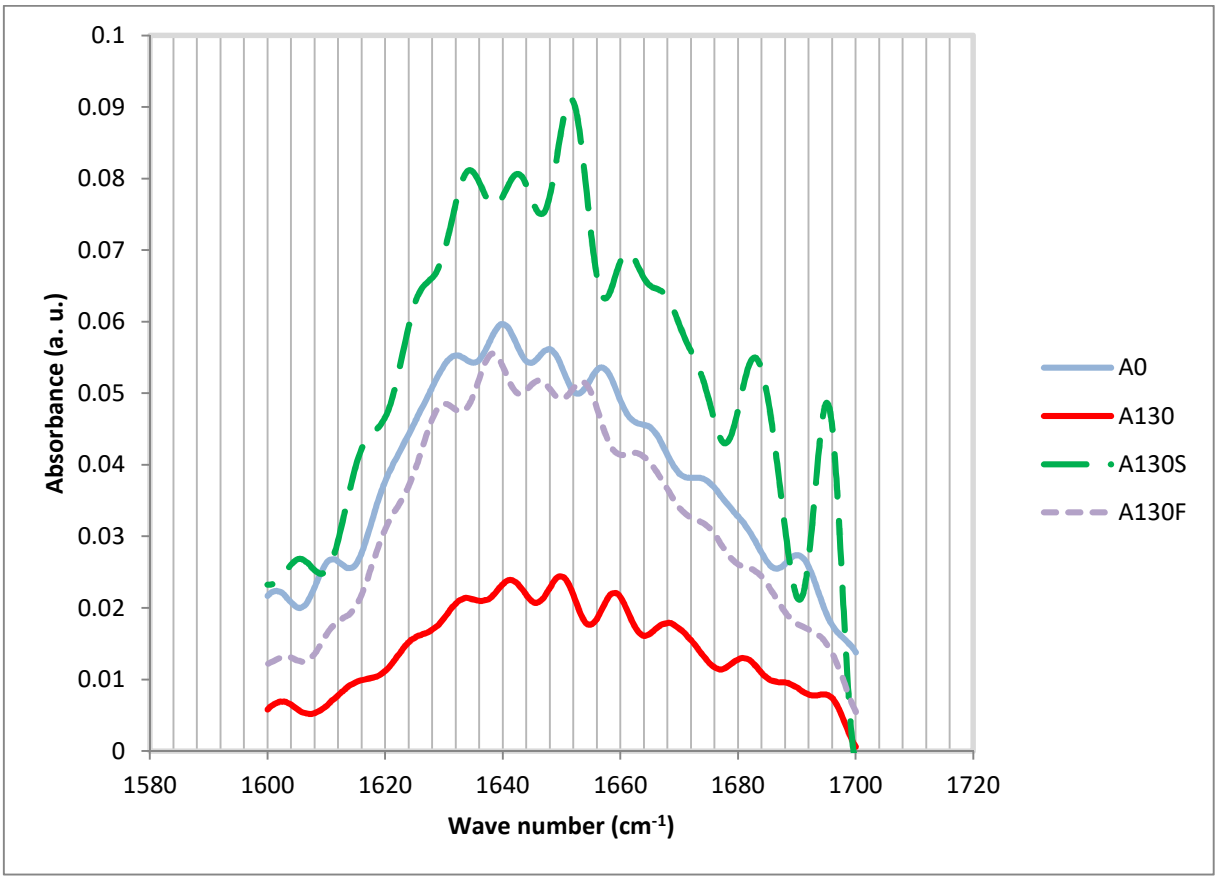

Figure 4.

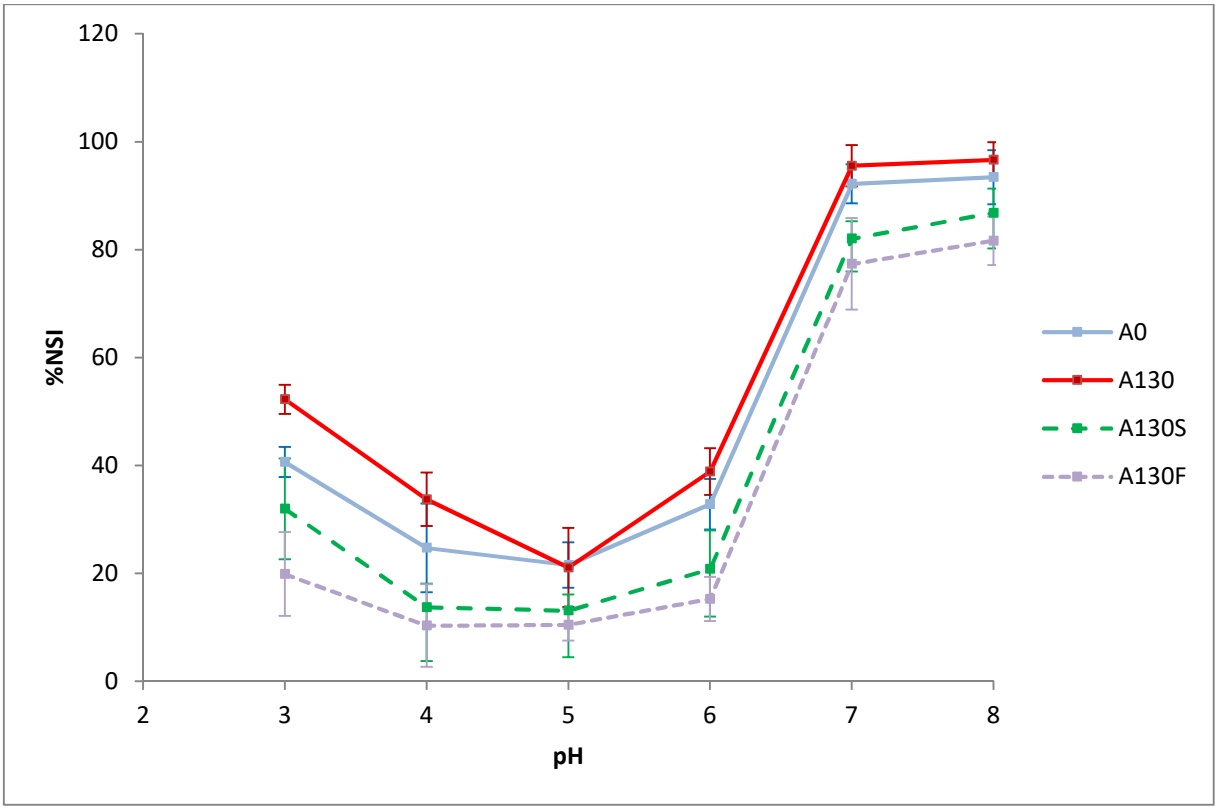

Figure 5.

a) A0

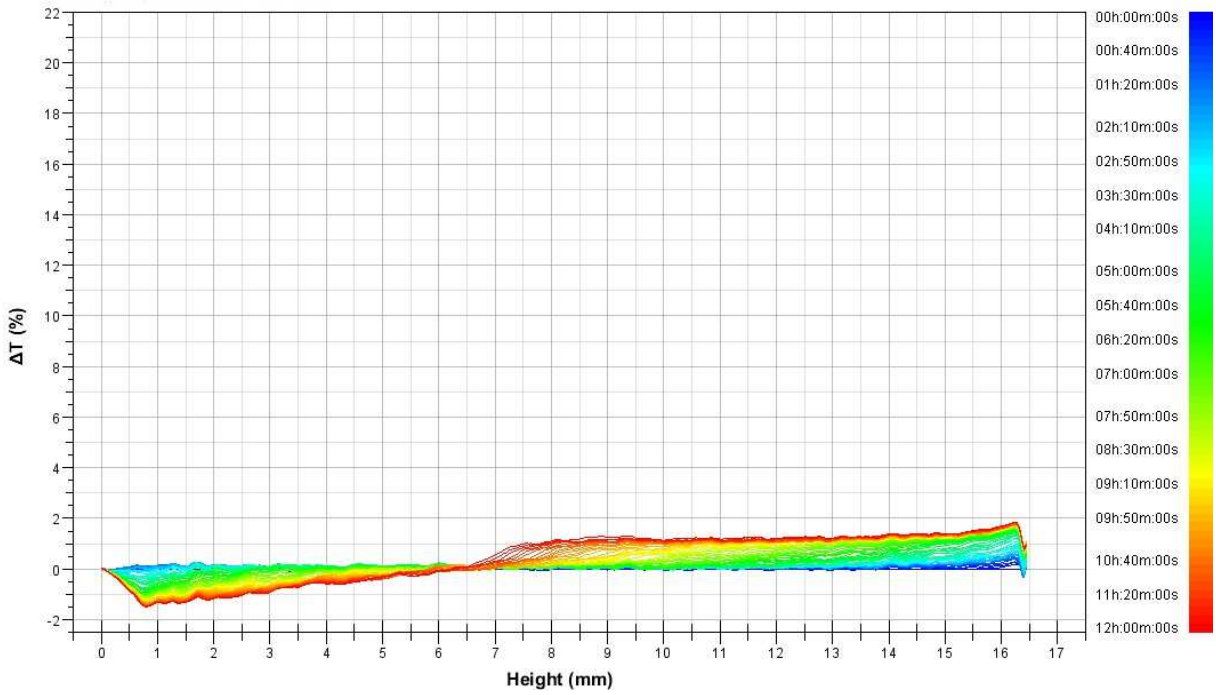

b) A130

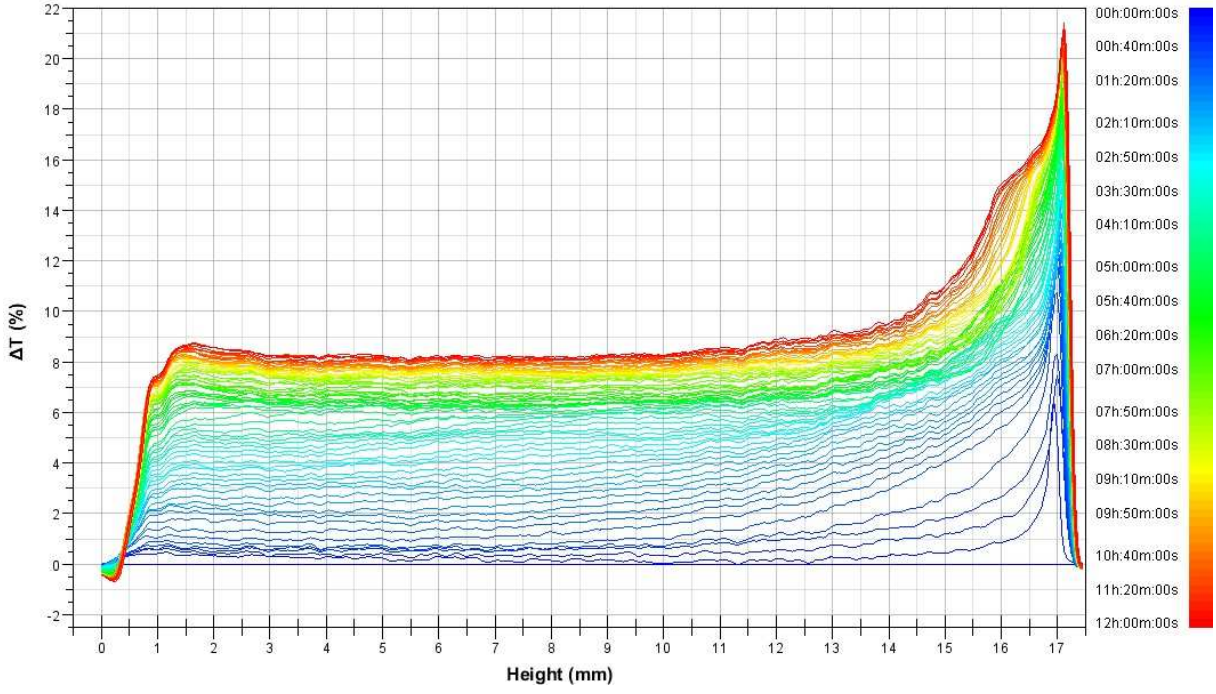

c) A130S

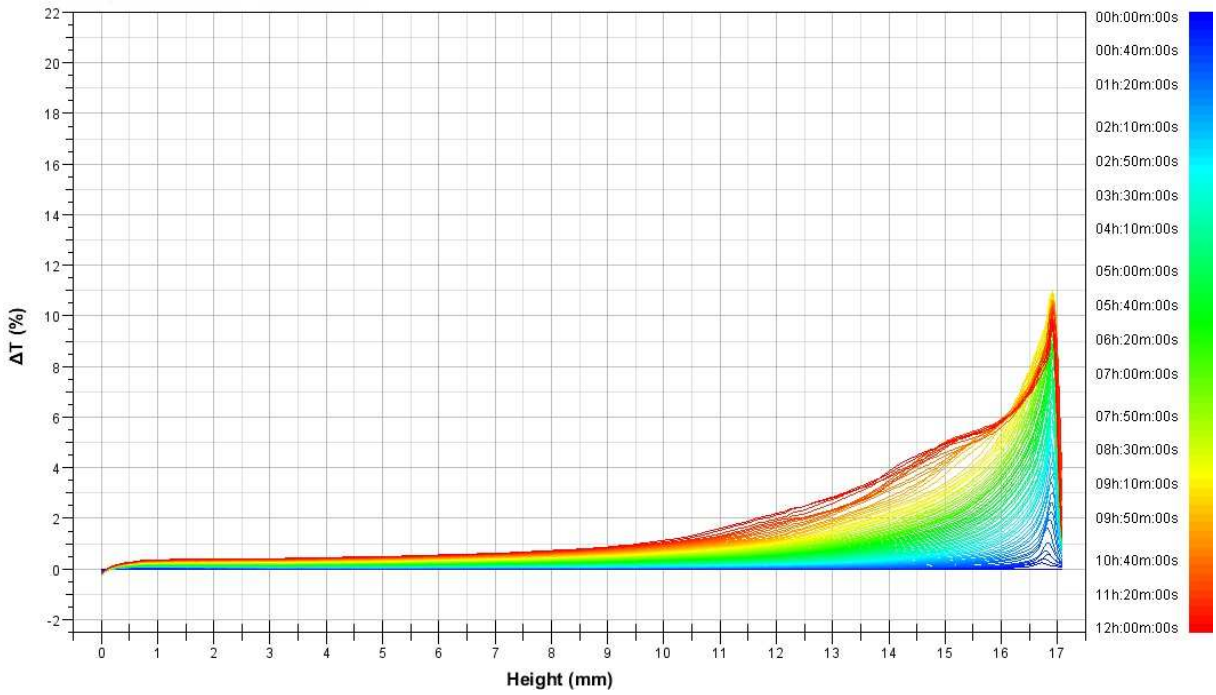

d) A130F

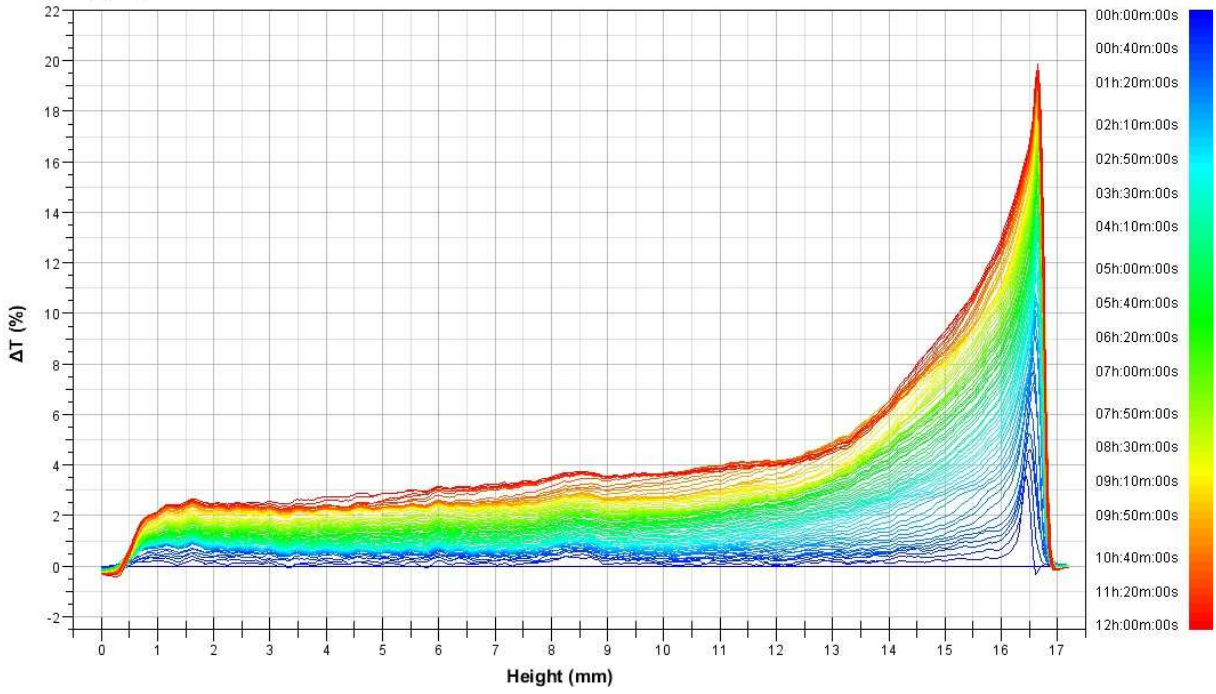

Figure 6.

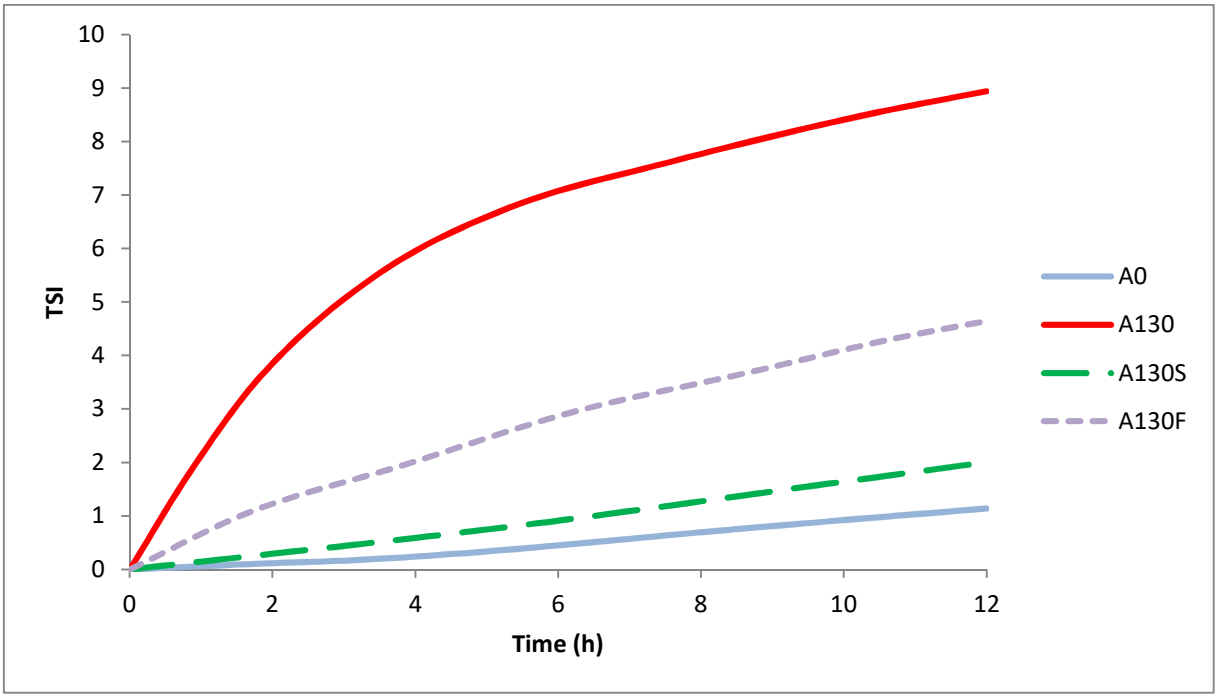
10
9
8
7
6
5
4
3
2
1
0
TSI
0
2
4
6
8
10
12
Time (h)
A0
A130
A130S
A130F

Tables

Table 1. Particle size distribution in terms of volume-average diameter (d4,3) and heterogeneity (Span) , surface hydrophobicity (H_o), and charge (ζ-potential) of pea globulin aggregates before microfluidization and drying (A0), after microfluidization at 130 MPa (A130), and after microfluidization and spray-drying (A130S) or freeze-drying (A130F) in 10 mM phosphate buffer at pH 7.2.

	d 4,3	Span	Ho	ζ-potential (mV)
A0	15.23 ± 2.37 c	95.48 ± 13.62 c	6007.00 ± 104.25 c	-13.53 ± 0.42 a
A130	4.11 ± 0.13 a	31.39 ± 1.36 b	5618.33 ± 70.57 b	-13.35 ± 0.87 a
A130S	5.59 ± 0.46 a	3.74 ± 0.24 a	3880.00 ± 18.03 a	-13.40 ± 0.94 a
A130F	11.90 ± 1.55 b	8.11 ± 0.60 a	3954.33 ± 18.72 a	-13.38 ± 0.51 a

Different superscripts in the same column represent significant differences among different samples (Tukey's *post hoc* test).

Table 2. Assignment of de-convoluted amide I bands in the FTIR spectrum of pea globulin aggregates before microfluidization and drying (A0), after microfluidization at 130 MPa (A130), and after microfluidization and spray-drying (A130S) or freeze-drying (A130F) in 10 mM phosphate buffer at pH 7.2

Assignment	Wavenumber (cm^{-1})			
	A0	A130	A130S	A130F
Vibration of amino acid residues	1602	1602	1605	1603
Anti-parallel β-sheet	1611	1614	1616	1612
Intermolecular hydrogen bonds in β-sheet	1622	1624	1625	1622
β-sheet	1632	1634	1635	1630
β-sheet	1639	1641	1643	1638
Random coil	1648	1650	1652	1646
α-helix	1657	1659	1661	1654
β-turns	1666	1668	1666	1662
β-turns	1682	1681	1683	1683
Aggregated strands	1691	1694	1695	1694

Pea Proteins

Thermal treatment

Pea Aggregates (PA)

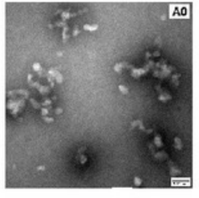

Microfluidization at 130 MPa

Microfluidized PA (MPA)

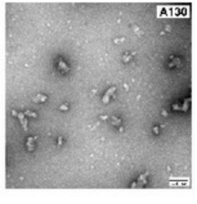

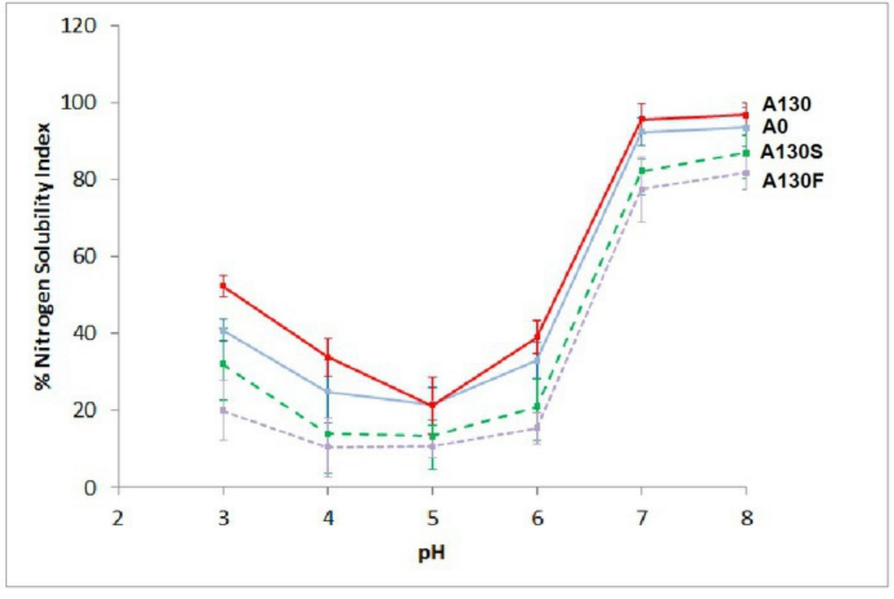

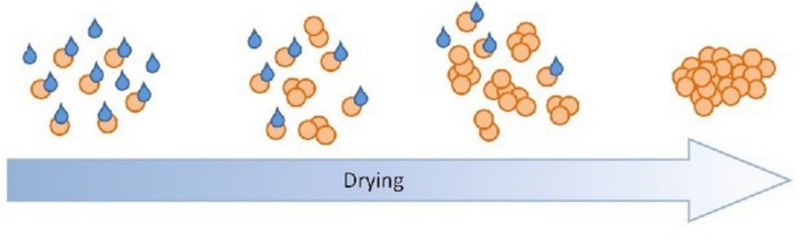

Spray-dried MPA

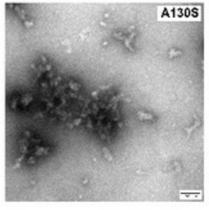

Freeze-dried MPA